Variational Monte Carlo calculations of $^{5}_{\Lambda}$He hypernucleus

A. A. Usmani*
Department of Physics, Aligarh Muslim University, Aligarh 202 002, India
and IUCAA, Ganeshkhind, Pune-411 007, India

S. Murtaza
Department of Physics, Aligarh Muslim University, Aligarh 202 002, India
(Received 23 February 2003; published 18 August 2003)

We perform a realistic study of $^{5}_{\Lambda}$He hypernucleus using variational Monte Carlo technique. The Hamiltonian for ^{4}He nuclear core of the hypernucleus is written using Argonne v_{18} NN potential and Urbana model-IX NNN potential, where N stands for nucleon. For the strange sector, we use phenomenological ΛN potential having central, spin, and exchange components and ΛNN potential which includes spin-dependent dispersive force and two-pion exchange force. Using this Hamiltonian and a fully correlated variational wave function, we reproduce the experimental Λ binding energy. Without three-body ΛNN potential in the Hamiltonian and its corresponding correlation in the wave function, the hypernucleus is overbound by 0.56(4) MeV, which is about a quarter of the previous reported values of 2–3 MeV due to the use of central forces. We present the detailed energy breakdown of the hypernucleus and also show the effect of ΛNN correlation on it. The one-body density profiles for nucleon and Λ in the hypernucleus and in its nuclear core have been critically examined. The nuclear core polarization due to presence of Λ is precisely determined.

DOI: 10.1103/PhysRevC.68.024001 PACS number(s): 21.80.+a, 21.10.Pc, 13.75.Ev, 13.75.Cs

I. INTRODUCTION

The $^{5}_{\Lambda}$He hypernucleus, a composite of four nucleons (N), and a distinguishable hyperon Λ with strangeness degree of freedom, has always been a focus of attraction for those studying strangeness physics of hypernuclei [1]. The Λ-separation energy in the ground state of this hypernucleus, because of the good experimental statistics, is the most reliable experimental information available to us in the hypernuclear laboratory. It has been, besides the ΛN scattering experiments and the hypernuclear decay, widely studied to bridge the gap in our fundamental understanding of baryon-baryon and three-baryon forces. It has also been used to explore the structure of the $^{5}_{\Lambda}$He. Although nucleons and hyperons are quark composites, at low energies quark and gluon degrees of freedom do not manifest themselves, and a description of baryon-baryon force using mesons works effectively. The question remains whether we can successfully calculate physical properties of such many-body systems in terms of realistic two- and three-baryon interactions without including the underlying QCD.

In this direction, some simplified microscopic calculations were performed for s-shell hypernuclei [2,3], a few p-shell hypernuclei [4], and Λ binding to nuclear matter [3,5]. But these studies were limited to central nucleon-nucleon (NN) interactions, which are far from the realistic picture of the hypernuclei. Also the Λ-nucleon (ΛN) potentials, parametrized to account for the various low energy scattering data and the binding energies of $^{3}_{\Lambda}$H, $^{4}_{\Lambda}$H, and $^{4}_{\Lambda}$He, overbind $^{5}_{\Lambda}$He hypernucleus, which is known as $A=5$ *anomaly* [2,6–8]. It was suggested [2,3] that the Λ-nucleon-nucleon (ΛNN) potential may resolve the overbinding problem. Besides, there were other attempts to resolve this problem by Bando and Shimodaya [9], and by Shinmura *et al.* [10], who had performed calculations under the framework of G matrix using Reid soft core and Hamada-Johnson NN potentials. At a later stage, detailed Monte Carlo studies of $^{17}_{\Lambda}$O hypernucleus using cluster Monte Carlo (CMC) [11] and $^{5}_{\Lambda}$He hypernucleus using variational Monte Carlo (VMC) [12] were carried out. In these two studies, the two-body NN and ΛN potentials were used in conjunction with the three-body NNN and ΛNN potentials. But the NN potential was the v_6, which represents the first six dominant terms of the Argonne v_{18} (AV18) potential [13]. In addition, all the correlations induced by these potentials were used to write the variational wave function under independent triplet approximation. The effect of ΛNN force and its corresponding correlation on energy breakdown, density profile, and nuclear core (NC) polarization was thoroughly investigated. However, for a detailed realistic study, one must include the neglected $v' = v_{18} - v_6$ terms.

In this paper, we use the full AV18 potential. We also improve the wave function through the inclusion of $\mathbf{L}\cdot\mathbf{S}$ and $\mathbf{L}\cdot\mathbf{S}\otimes(\boldsymbol{\tau}_1\cdot\boldsymbol{\tau}_2)$ correlations and incorporate other considerations for NC as by Pudliner *et al.* [14, 15] given in Sec. III.

II. THE HAMILTONIAN

We calculate the Λ separation energy

$$B_\Lambda = \frac{\langle \Psi_{NC}|H_{NC}|\Psi_{NC}\rangle}{\langle \Psi_{NC}|\Psi_{NC}\rangle} - \frac{\langle \Psi|H|\Psi\rangle}{\langle \Psi|\Psi\rangle}, \tag{1}$$

where $\Psi(\Psi_{NC})$ and $H(H_{NC})$ are used to refer to the ground state wave function and Hamiltonian of hypernucleus (isolated $A-1$ bound nucleons).

*Email address: anisul@bharatmail.com

The nonrelativistic Hamiltonian of an A-baryon hypernucleus containing $A-1$ nucleons and a Λ baryon is

$$H = H_{NC} + H_{\Lambda}, \tag{2}$$

where H_{NC} is the nuclear core Hamiltonian,

$$H_{NC} = \sum_{i}^{A-1} \frac{p_i^2}{2m} + \sum_{i<j}^{A-1} v_{ij} + \sum_{i<j<k}^{A-1} V_{ijk}, \tag{3}$$

and

$$H_{\Lambda} = T_{\Lambda} + \sum_{i=1}^{A-1} v_{\Lambda i} + \sum_{i<j}^{A-1} V_{\Lambda ij} \tag{4}$$

is the part of the energy due to presence of Λ. In these expressions, v_{ij} and V_{ijk} are NN and NNN potentials. For NN potential we use AV18, which is written as a sum of 18 terms,

$$v_{ij} = \sum_{p=1,18} v_p(r_{ij}) O_{ij}^p, \tag{5}$$

where the first 14 terms are charge independent,

$$O_{ij}^{p=1,14} = [1, \boldsymbol{\sigma}_i \cdot \boldsymbol{\sigma}_j, S_{ij}, \mathbf{L}\cdot\mathbf{S}, \mathbf{L}^2, \mathbf{L}^2 \boldsymbol{\sigma}_i \cdot \boldsymbol{\sigma}_j, (\mathbf{L}\cdot\mathbf{S})^2] \otimes [1, \boldsymbol{\tau}_i \cdot \boldsymbol{\tau}_j], \tag{6}$$

and the rest,

$$O_{ij}^{p=15,18} = [1, \boldsymbol{\sigma}_i \cdot \boldsymbol{\sigma}_j, S_{ij}] \otimes T_{ij}, (\boldsymbol{\tau}_{zi} + \boldsymbol{\tau}_{zj}), \tag{7}$$

are charge independence breaking terms. For the NNN potential, we use Urbana-IX (UIX) model of the Urbana series potentials [16]. This has a long range two-pion exchange component and a short range phenomenological component, written as

$$V_{ijk} = V_{ijk}^{2\pi} + V_{ijk}^{R}. \tag{8}$$

We use these in conjunction with the ΛN and ΛNN potentials, which are represented by $V_{\Lambda i}$ and $V_{\Lambda ij}$ in Eq. (4).

A. The ΛN potential

Unlike the NN interaction, single-pion exchange is forbidden in ΛN interaction. The two-pion exchange (TPE) is a dominant part of the ΛN potential that is determined by the strong tensor one-pion-exchange (OPE) component acting twice. The tensor part of the ΛN interaction is very weak because the short range $\overline{K}$ and K^* exchanges that are responsible for this are of opposite sign and nearly cancel each other. Moreover, there is the K exchange interaction that primarily contributes to the ΛN exchange potential.

We use an Urbana type charge symmetric potential [4,17] with spin and space exchange components, and a TPE tail which is consistent with Λp scattering below the Σ threshold,

$$v_{\Lambda N}(r) = v_0(r)(1 - \varepsilon + \varepsilon P_x) + \tfrac{1}{4} v_{\sigma} T_{\pi}^2(r) \boldsymbol{\sigma}_{\Lambda} \cdot \boldsymbol{\sigma}_N, \tag{9}$$

$$v_0 = v_c(r) - \overline{v} T_{\pi}^2(r), \tag{10}$$

$$v_c = \frac{W_c}{1 + \exp(r-R)/a}. \tag{11}$$

Here $T_{\pi}(r)$ is the OPE tensor potential

$$T_{\pi} = \left(1 + \frac{3}{\mu r} + \frac{3}{(\mu r)^2}\right) \frac{\exp(-\mu r)}{\mu r} [1 - \exp(-cr^2)]^2, \tag{12}$$

with $\mu = 0.7$ fm^{-1}, and the cutoff parameter $c = 2.0$ fm^{-2}. P_x is the space-exchange operator and ε is the corresponding exchange parameter. The $\overline{v} = (v_s + 3v_t)/4$ and $v_{\sigma} = v_t - v_s$ are, respectively, the spin-average and spin-dependent strengths, where v_s and v_t denote singlet- and triplet-state depths, respectively. The spin dependence in Eq. (9) is found to be negligibly small [11,12] in ${}^{5}_{\Lambda}$He and ${}^{17}_{\Lambda}$O. The $v_c(r)$ is a short range Woods-Saxon repulsive potential. The various parameters are

$$v_s = 6.33 \text{ MeV}, \quad v_t = 6.1 \text{ MeV}, \quad \varepsilon = 0.3,$$

$$W_c = 2137 \text{ MeV}, \quad R = 0.5 \text{ fm}, \quad a = 0.2 \text{ fm}.$$

These parameters are consistent with the low energy Λp scattering data that essentially determine the spin-average potential $\overline{v}$. The parameter ε for the space-exchange strength is fairly well determined from the Λ single-particle scattering data [18,19]. One may also add a charge symmetry breaking term in Eq. (9), which may give significant result at large values of A with a substantial neutron excess [18,20].

B. The ΛNN potential

The ΛN force as obtained by fitting the Λp scattering does not provide a good account of the experimental binding energies. The other considerations such as many-body effects and the suppression of the tensor force by the medium are small [18,21], in order to reproduce the experimental binding energies. However, we note herein that a fully realistic description of NC narrows the gap between theory and experiment significantly. But we still require a three-body TPE ΛNN force to resolve the overbinding. Unlike the ΛN potential, the ΛNN potential may be strongly suppressed because of the modifications of the propagation of intermediate hyperonic state. The intermediate hyperonic state can be a Σ as well as any of the $(I=1, S=-1)$ Σ^* resonances. The first such resonance is a $\pi\Lambda$ resonance $\Sigma^*(1385)$, analogous to $N^*(1236)$ in the πN system. In order for the diagrams given in Fig. 1 to be operative, each nucleon must be localized within a fairly large distance of $\hbar/m_{\pi}c \approx 1.4$ fm from the Λ particle. The other calculations show a repulsive contribution suggested by the suppression mechanism due to ΛN-ΣN coupling [22,23]. Corresponding to both the diagrams of Fig.

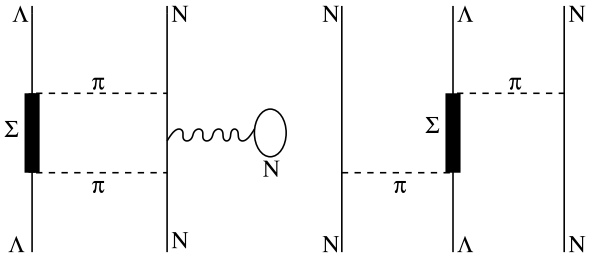

FIG. 1. Diagrams contributing to ΛNN potential.

1, one may write two Wigner types of ΛNN forces, namely, the dispersive ΛNN force and the TPE ΛNN force.

The repulsive ''dispersive'' force is written in phenomenological form with an explicit spin dependence [3] as

$$V^{D}_{\Lambda NN}=W_0 T^2_{\pi}(r_{\Lambda 1})T^2_{\pi}(r_{\Lambda 2})[1+\tfrac{1}{6}\boldsymbol{\sigma}_{\Lambda}\cdot(\boldsymbol{\sigma}_1+\boldsymbol{\sigma}_2)], \tag{13}$$

where W_0 is the strength of the potential and $T_{\pi}(r_{\Lambda i})$ is given by Eq. (12). For the spin-zero core, the second term in the square brackets is practically zero.

In principle, TPE arises from *p*- and *s*-wave pion interactions of the Λ with nucleons, but the latter is negligibly small. Therefore, TPE may fairly be described as a *p*-wave $\pi\Lambda$ interaction [6,24], which is written as

$$V^{2\pi}_{\Lambda NN}=-\left(\frac{C_p}{6}\right)(\boldsymbol{\tau}_1\cdot\boldsymbol{\tau}_2)\{X_{\Lambda 1},X_{\Lambda 2}\}. \tag{14}$$

Here

$$X_{\Lambda i}=(\boldsymbol{\sigma}_{\Lambda}\cdot\boldsymbol{\sigma}_i)Y_{\pi}(r_{\Lambda i})+S_{\Lambda i}T_{\pi}(r_{\Lambda i}), \tag{15}$$

$$Y_{\pi}(r)=\frac{\exp(-\mu r)}{\mu r}[1-\exp(-cr^2)] \tag{16}$$

is the OPE Yukawa function, and C_p is the strength of the potential.

III. THE VARIATIONAL WAVE FUNCTION

The variational wave function [25] for nuclei may be generalized to write the wave function for $^{5}_{\Lambda}$He hypernucleus,

$$|\Psi\rangle=\left[1+\sum_{j<k}^{A-1}U_{\Lambda jk}+\sum_{i<j<k}^{A-1}(U_{ijk}+U^{TNI}_{ijk})+\sum_{i<j}U^{LS}_{ij}\right]|\Psi_p\rangle, \tag{17}$$

where the pair wave function Ψ_p is written as

$$|\Psi_p\rangle=\left[\prod_{j=1}^{A-1}(1+U_{\Lambda j})\right]\left[S\prod_{i<j}^{A-1}(1+U_{ij})\right]|\Psi_J\rangle. \tag{18}$$

Here U_{ij}, U^{LS}_{ij}, $U_{\Lambda j}$, U_{ijk}, U^{TNI}_{ijk}, and $U_{\Lambda jk}$ are the noncommuting two- and three-baryon correlation operators. *S* is a symmetrization operator. $|\Psi_J\rangle$ is the antisymmetric Jastrow wave function,

$$|\Psi_J\rangle=\left[\prod_{j<k}^{A-1}f^{c}_{\Lambda jk}(r_{\Lambda jk})\right]\left[\prod_{j=1}^{A-1}f^{c}_{\Lambda}(r_{\Lambda j})\right]\left[\prod_{i<j<k}^{A-1}f^{c}_{ijk}(r_{ijk})\right]\times\left[\prod_{i<j}^{A-1}f^{c}_{ij}(r_{ij})\right]\mathcal{A}|\phi^{A-1}\rangle. \tag{19}$$

Here, $f^{c}_{ij}(r_{ij})$ and $f^{c}_{\Lambda}(r_{\Lambda j})$ are central correlations that are primarily generated by the repulsive core in the two-baryon interactions, f^{c}_{ijk} and $f^{c}_{\Lambda jk}$ are the central three-body correlation functions, and

$$\mathcal{A}|\Phi^{A-1}\rangle=\mathcal{A}[(n\uparrow)_1(n\downarrow)_2(p\uparrow)_3(p\downarrow)_4], \tag{20}$$

where $\mathcal{A}$ is the antisymmetrization operator running over nucleons.

U_{ij} is a sum of spin, isospin, and tensor operators,

$$U_{ij}=\sum_{p=2,6}\left[\prod_{k\neq i,j}f^{p}_{ijk}(\mathbf{r}_{ik}\cdot\mathbf{r}_{jk})\right]u_p(r_{ij})O^{p}_{ij}, \tag{21}$$

and U^{LS}_{ij} is the spin-orbit correlation operator,

$$U^{LS}_{ij}=\sum_{p=7,8}u_p(r_{ij})O^{p}_{ij}, \tag{22}$$

with

$$O^{p=1,8}_{ij}=[1,\boldsymbol{\sigma}_i\cdot\boldsymbol{\sigma}_j,S_{ij},(\mathbf{L}\cdot\mathbf{S})_{ij}]\otimes[1,\boldsymbol{\tau}_i\cdot\boldsymbol{\tau}_j]. \tag{23}$$

The functions $f_c(r_{ij})$ and $u_p(r_{ij})$ are the same as given in Ref. [26]. The three-nucleon correlations induced by v_{ij} are discussed in Ref. [14] and references therein. Their explicit mathematical expressions are

$$f^{c}_{ijk}=1+q^{c}_1(\mathbf{r}_{ij}\cdot\mathbf{r}_{ik})(\mathbf{r}_{ji}\cdot\mathbf{r}_{jk})(\mathbf{r}_{ki}\cdot\mathbf{r}_{kj})\exp(-q^{c}_2R_{ijk}), \tag{24}$$

$$f^{p}_{ijk}=1-q^{p}_1(1-\hat{\mathbf{r}}_{ij}\cdot\hat{\mathbf{r}}_{jk})\exp(-q^{p}_2R_{ijk}), \tag{25}$$

and U_{ijk} is a complicated operatorial combination as discussed in Ref. [25]. U^{TNI}_{ijk} is the three-nucleon correlation induced by the three-nucleon interaction, which is written in the form [14]

$$U^{TNI}_{ijk}=\sum_{x=R,A,C}\epsilon_x V^{x}_{ijk}(\tilde{r}_{ij},\tilde{r}_{jk},\tilde{r}_{ki}), \tag{26}$$

where *r* is scaled through a parameter *y* as

$$\tilde{r}=yr, \tag{27}$$

and $\epsilon_x(x=A,C,R)$ is the strength parameter for the three different terms of the *NNN* potential [27].

For $U_{\Lambda j}$, we choose

$$U_{\Lambda j}=\sum_{p=2,3}\left[\prod_{k\neq j}f^{p}_{\Lambda jk}(\mathbf{r}_{\Lambda k}\cdot\mathbf{r}_{jk})\right]u_p(r_{\Lambda j})O^{p}_{\Lambda j}, \tag{28}$$

with

$$O_{\Lambda j}^{p=1,3}=[1,\boldsymbol{\sigma}_\Lambda\cdot\boldsymbol{\sigma}_j,P_x], \tag{29}$$

where P_x is the exchange operator and

$$u_\sigma^\Lambda=\frac{f_\Lambda^t-f_\Lambda^s}{f_\Lambda^c}. \tag{30}$$

We may also generalize f_{ijk}^c and f_{ijk}^p for ΛNN three-body correlations, $f_{\Lambda jk}^c$ and $f_{\Lambda jk}^p$ as

$$f_{\Lambda jk}^c=1+z_1^c(\mathbf{r}_{\Lambda j}\cdot\mathbf{r}_{\Lambda k})(\mathbf{r}_{j\Lambda}\cdot\mathbf{r}_{jk})(\mathbf{r}_{k\Lambda}\cdot\mathbf{r}_{kj})\exp(-z_2^cR_{\Lambda jk}), \tag{31}$$

$$f_{\Lambda jk}^p=1-z_1^p(1-\hat{\mathbf{r}}_{\Lambda j}\cdot\hat{\mathbf{r}}_{jk})\exp(-z_2^pR_{\Lambda jk}). \tag{32}$$

The $f_\Lambda^{s(t)}$ is the solution of the Schrödinger equation

$$\left[\frac{-\hbar^2}{2\mu_{\Lambda N}}\nabla^2+\tilde{v}_{s(t)}(r_{\Lambda N})+\theta_{\Lambda N}\right]f_\Lambda^{s(t)}=0, \tag{33}$$

with quenched ΛN potentials in singlet and triplet states,

$$\tilde{v}_s(r)=v_c(r)-(\alpha_{2\pi}\overline{v}+\tfrac{3}{4}\alpha_\sigma v_\sigma)T_\pi^2(r),$$

$$\tilde{v}_t(r)=v_c(r)-(\alpha_{2\pi}\overline{v}-\tfrac{1}{4}\alpha_\sigma v_\sigma)T_\pi^2(r). \tag{34}$$

The spin-averaged correlation function is defined as

$$f_\Lambda^c=\frac{f_\Lambda^s+3f_\Lambda^t}{4}, \tag{35}$$

and following Ref. [3], the auxiliary potential $\theta_{\Lambda N}$ may be written as

$$\theta_{\Lambda N}=\frac{\hbar^2}{2\mu_{\Lambda N}}\left(\kappa_{\Lambda N}^2-\frac{2\kappa_{\Lambda N}(\nu_{\Lambda N}-1)}{r}+\frac{\nu_{\Lambda N}(\nu_{\Lambda N}-1)}{r^2}\right)\times\left(1-\exp\frac{-r^2}{C_{\Lambda N}^2}\right)+\frac{\gamma_{\Lambda N}}{1+\exp\left(\dfrac{r-R_{\Lambda N}}{a_{\Lambda N}}\right)}, \tag{36}$$

which ensures the asymptotic behavior

$$f_{\Lambda N}^c\sim r^{-\nu_{\Lambda N}}e^{-\kappa_{\Lambda N}r} \tag{37}$$

required by the Eq. (33).

The $U_{\Lambda jk}$ involved in Eq. (17) have the same structure as their corresponding interaction,

$$U_{\Lambda jk}=\sum_{x=D,2\pi}\epsilon_x^\Lambda V_{\Lambda jk}^x(\tilde{r}_{\Lambda j},\tilde{r}_{jk},\tilde{r}_{k\Lambda}), \tag{38}$$

with

$$\tilde{r}=y_\Lambda r \tag{39}$$

and $\epsilon_{x=D,2\pi}^\Lambda$, which stands for both D (repulsive) and 2π (attractive) components of the ΛNN potential. In other words $U_{\Lambda jk}$ differs with $V_{\Lambda jk}$ through the range c of the cutoff functions $T_\pi(r)$ and $Y_\pi(r)$ as given below,

$$\tilde{c}=cy_\Lambda^2. \tag{40}$$

TABLE I. Values of asymptotic parameters used to generate trial wave function for the NC of $^5_\Lambda$He. The ^{4}He parameters and notations are the same as Refs. [14,26]. The parameters which remain unchanged for $^5_\Lambda$He are not listed here.

	NC	^{4}He
$E_{0,0}$ (MeV)	14.0	17.0
$E_{0,1}$ (MeV)	16.0	16.0
$E_{1,0}$ (MeV)	21.5	23.5
$E_{1,1}$ (MeV)	12.0	16.5
η_0	0.36	0.35

IV. RESULTS AND DISCUSSION

A. Variational parameters

All calculations are carried out using the Hamiltonian consisting of ΛN, ΛNN, NN (AV18), and NNN (UIX) interactions. The variational searches have been performed for two cases: (i) with $U_{\Lambda jk}$ that implicitly involves ΛNN potential strengths W_0 and C_p through Eq. (38) and (ii) without $U_{\Lambda jk}$ and $V_{\Lambda jk}$.

The best values of the parameters that describe the ^{4}He nucleus are due to Pudliner *et al.* [14] and Wiringa [26]. Using these parameters the ground state energy of ^{4}He nucleus is estimated to be $-27.73(2)$ MeV. The number in parentheses is the error in the last digit. The wave function describing the NC need not necessarily be the same as ^{4}He nucleus due to the presence of Λ hyperon in the hypernucleus. We do notice that some of these parameters need to be changed for an optimal variational wave function. Values of asymptotic parameters used to generate trial wave function for NC and ^{4}He are given in Table I and the three-nucleon correlation parameters are listed in Table II. The noncentral NN correlations are obtained through the quenched potential strengths. These quenching factors are

TABLE II. Values of three-nucleon correlation parameters. The ^{4}He parameters and notations are the same as Refs. [14,26]. The parameters which remain unchanged for $^5_\Lambda$He are not listed here.

	NC	^{4}He
ϵ_R	-0.00027	-0.00025
ϵ_C	-0.0005	-0.0004
y	0.73	0.72
q_1^c (fm^{-6})	0.18	0.20
q_2^c (fm^{-1})	0.80	0.85
$q_1^{\ell s}$ (fm^{-2})	-0.10	-0.12
$q_2^{\ell s}$ (fm^{-2})	0.11	0.12
$q_3^{\ell s}$ (fm^{-2})	0.80	0.85
q_3^τ (fm)	1.25	1.20

TABLE III. Noncentral potential quenching factors for NN correlation functions.

	NC	^{4}He
α_2	0.93	0.93
α_3	0.92	0.92
α_4	0.92	0.92
α_5	0.82	0.86
α_6	0.82	0.85
α_7	0.80	0.80
α_8	0.80	0.80

listed in Table III. The best asymptotic parameters used to generate long range ΛN correlation are given in Table IV.

Similarly, the ΛN correlation functions are also obtained through the quenched potentials as in Eq. (34). These are

$$\alpha^{\Lambda}_{2\pi}=0.935, \quad \alpha^{\Lambda}_{\sigma}=0.70. \tag{41}$$

$\gamma_{\Lambda N}$ is determined by matching the logarithmic derivative at a suitable r. In addition to these, the tuned parameters for the $U_{\Lambda NN}$ correlation for the strengths $W_0=0.012$ MeV and $C_p=0.75$ MeV are

$$\begin{aligned} \epsilon^{\Lambda}_{D}&=-0.00163, \\ \epsilon^{\Lambda}_{2\pi}&=-0.0016. \end{aligned} \tag{42}$$

We also note that both the variational parameters, z^c_1 and z^p_1, in Eqs. (31) and (32) are setting to zero, thereby giving a simple form for the operator independent three-body correlations as follows:

$$f^{c}_{\Lambda jk}=f^{p}_{\Lambda jk}=1. \tag{43}$$

The optimal value of y_Λ is found to be 0.81 fm^{-1}. These parameters give the Λ-separation energy which is very close to the experiment.

We note a linear behavior for $\langle V^D_{\Lambda NN}\rangle$ with respect to W_0 (Fig. 2) with a slope

$$\frac{dV^D_{\Lambda NN}}{dW_0}\approx 164. \tag{44}$$

However, dependence of $V^{2\pi}_{\Lambda NN}$ with respect to C_p is quadratic, which is attributed to the $U_{\Lambda NN}$ correlation. These results confirm the old studies [11,12]. As both $\langle V^D_{\Lambda NN}\rangle$ and $\langle V^{2\pi}_{\Lambda NN}\rangle$ are opposite in sign, different combinations of W_0 and C_p may reproduce the experimental Λ-separation energy 3.12(2) MeV. However, as obvious from Eq. (38), any change brought to W_0 and C_p will offset the optimal variational wave function obtained for $W_0=0.012$ MeV and $C_p=0.75$ MeV. In order to retain the same wave function, therefore, we must reset the values of ϵ^{Λ}_{D} and $\epsilon^{\Lambda}_{2\pi}$ accordingly using

$$\begin{aligned} \epsilon^{\Lambda}_{D}&=-\frac{0.012(0.00163)}{W_0}, \\ \epsilon^{\Lambda}_{2\pi}&=-\frac{0.75(0.0016)}{C_p}. \end{aligned} \tag{45}$$

TABLE IV. Values of asymptotic parameters used to generate long range ΛN correlation function.

$\kappa_{\Lambda N}$	0.008 (fm^{-1})
$\nu_{\Lambda N}$	0.62
$C_{\Lambda N}$	3.5 (fm^{-1})
$a_{\Lambda N}$	0.6 (fm)
$R_{\Lambda N}$	0.35 (fm)

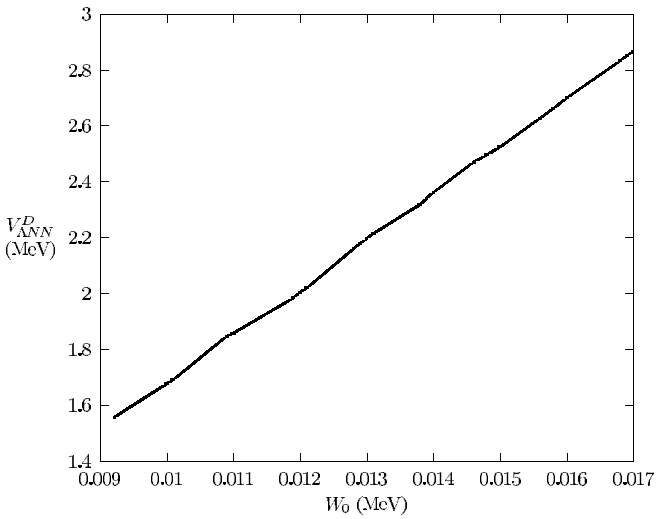

FIG. 2. Dependence of $\langle V^D_{\Lambda NN}\rangle$ on W_0.

B. Variational energies

As mentioned before, the old variational Monte Carlo calculations of $^{17}_{\Lambda}$O [11] and $^{5}_{\Lambda}$He [12] hypernuclei were carried out using the truncated v_6 NN potential along with their corresponding NN correlations. The variational wave function too was written without $U^{LS}_{ij}(\mathbf{L}\cdot\mathbf{S})\otimes(1,\boldsymbol{\tau}_1\cdot\boldsymbol{\tau}_2)$ correlations and with simplified triplet correlation. In the present study, the calculations have been improved by incorporating the full AV18 potential and by writing a more general variational wave function that involves additional $U^{LS}_{ij}(\mathbf{L}\cdot\mathbf{S})\otimes(1,\boldsymbol{\tau}_1\cdot\boldsymbol{\tau}_2)$ two-body correlations along with full three-body U_{ijk} and U^{TNI}_{ijk} correlations as in Eq. (17).

We compare our results obtained for the strengths $W_0=0.015$ MeV and $C_p=0.6$ MeV with the old results (Ref. [12]) obtained for the same strengths which were fixed to reproduce the experimental B_Λ value but with v_6 NN potential and correlations induced by v_6. Herein, we underestimate the Λ-separation energy by 1.02(4) MeV. This loss of the B_Λ value is attributed to the differences of NN potential and variational wave function between the two studies, which we analyze as follows: (i) the effect of $U^{LS}_{ij}(\mathbf{L}\cdot\mathbf{S})\otimes(1,\boldsymbol{\tau}_1\cdot\boldsymbol{\tau}_2)$ correlations to the B_Λ is found to be 0.16(2) MeV as its contributions in ^{4}He and in $^{5}_{\Lambda}$He are $-0.41(1)$ MeV and $-0.25(1)$ MeV, respectively, (ii) the contribution

TABLE V. Variational results for $V^D_{\Lambda NN}$, $V^{2\pi}_{\Lambda NN}$, and B_Λ. All quantities are in units of MeV.

C_p	W_0	$V^D_{\Lambda NN}$	$V^{2\pi}_{\Lambda NN}$	$V_{\Lambda NN}$	$E(^5_\Lambda\mathrm{He})$	B_Λ
1.0	0.0168	2.83(2)	−3.25(3)	−0.42(2)	−30.84(2)	3.11(4)
	0.0169	2.85(2)	−3.25(3)	−0.40(2)	−30.82(2)	3.09(4)
	0.0170	2.86(2)	−3.25(3)	−0.38(2)	−30.81(2)	3.08(4)
0.95	0.0156	2.63(2)	−3.10(3)	−0.47(2)	−30.89(2)	3.16(4)
	0.0158	2.66(2)	−3.08(3)	−0.42(2)	−30.86(2)	3.13(4)
	0.0160	2.70(2)	−3.08(3)	−0.38(2)	−30.80(2)	3.08(4)
0.90	0.0146	2.47(2)	−2.90(3)	−0.44(2)	−30.87(2)	3.14(4)
	0.0148	2.50(2)	−2.95(3)	−0.44(2)	−30.86(2)	3.13(4)
	0.0150	2.53(2)	−2.93(3)	−0.39(2)	−30.81(2)	3.08(4)
0.85	0.0138	2.31(2)	−2.74(2)	−0.43(2)	−30.87(2)	3.14(4)
	0.0139	2.34(2)	−2.74(2)	−0.41(2)	−30.85(2)	3.12(4)
	0.0140	2.36(2)	−2.74(2)	−0.40(2)	−30.83(2)	3.10(4)
0.80	0.0129	2.18(2)	−2.61(2)	−0.44(2)	−30.88(2)	3.15(4)
	0.0130	2.20(2)	−2.61(2)	−0.41(2)	−30.86(2)	3.13(4)
	0.0131	2.22(2)	−2.60(2)	−0.38(2)	−30.82(2)	3.09(4)
0.75	0.0119	1.98(1)	−2.42(2)	−0.44(2)	−30.85(2)	3.12(4)
	0.0120	1.99(1)	−2.42(2)	−0.42(2)	−30.84(2)	3.11(4)
	0.0121	2.02(1)	−2.42(2)	−0.40(2)	−30.83(2)	3.10(4)
0.70	0.0109	1.85(1)	−2.29(2)	−0.43(2)	−30.87(2)	3.14(4)
	0.0110	1.86(1)	−2.29(2)	−0.42(1)	−30.85(2)	3.12(4)
0.65	0.0100	1.68(1)	−2.12(2)	−0.43(1)	−30.86(2)	3.13(4)
	0.0101	1.69(1)	−2.12(2)	−0.42(1)	−30.84(2)	3.11(4)
0.60	0.0092	1.56(1)	−1.97(2)	−0.41(1)	−30.81(2)	3.08(4)

of v' (the difference between AV18 and v_6 NN potential) to the B_Λ is found by about 0.7(1) MeV as its expectation value for ^{4}He is 0.45(2) MeV and for $^5_\Lambda$He is 1.15(6) MeV, and (iii) the small residual contribution is attributed to the other changes in the variational wave function.

This loss in the separation energy may be compensated through the ΛNN potential either by decreasing the repulsive strength W_0 or by increasing the attractive strength C_p. We do both. A summary of B_Λ for different combinations of W_0 and C_p strengths is reported in Table V. The $\langle V^D_{\Lambda NN}\rangle$

TABLE VI. Energy breakdown for $^5_\Lambda$He hypernucleus. All quantities are in units of MeV.

		With $U_{\Lambda ij}$	With no $U_{\Lambda ij}$ and $V_{\Lambda ij}$
Λ Kinetic energy	T_Λ	7.98(3)	9.45(3)
	$v_0(r)(1-\epsilon)$	−11.76(4)	−13.91(5)
	$v_0(r)\epsilon P_x$	−4.39(2)	−5.30(2)
	$\frac{1}{4}v_\sigma T^2_\pi \boldsymbol{\sigma}_\Lambda\cdot\boldsymbol{\sigma}_N$	0.05	0.06
ΛN Potential energy	$V_{\Lambda N}$	−16.19(6)	−19.27(7)
	$V^D_{\Lambda NN}$ (W_0=0.012 MeV)	1.99(1)	
	$V^{2\pi}_{\Lambda NN}$ (C_p=0.75 MeV)	−2.41(2)	
ΛNN Potential energy	$V_{\Lambda NN}=V^D_{\Lambda NN}+V^{2\pi}_{\Lambda NN}$	−0.44(1)	
Λ Potential energy	$v_{\Lambda N}+V_{\Lambda NN}$	−16.63(6)	−19.27(7)
Total Λ energy	$E_\Lambda=T_\Lambda+v_{\Lambda N}+V_{\Lambda NN}$	−8.65(9)	−9.82(7)
NC Kinetic energy	T_{NC}	114.34(22)	117.51(22)
	v_6	−131.99(21)	−134.49(21)
	v_{NN}	−130.84(19)	−133.38(20)
	V_{NNN}	−5.68(2)	−5.75(2)
NC Potential energy	$V_{NC}=v_{NN}+V_{NNN}$	−136.52(21)	−139.13(20)
NC Energy	$E_{NC}=T_{NC}+V_{NC}$	−22.18(6)	−21.62(6)
$^5_\Lambda$He Energy		−30.84(2)	−31.41(3)
Λ Separation energy	B_Λ	3.11(4)	3.68(5)

TABLE VII. NC polarization. All quantities are in units of MeV.

	NC	^{4}He	Polarization
$T_{NC}^{internal}$	111.97(22)	107.31(21)	4.66(43)
v_{NN}	−130.84(21)	−129.81(21)	−1.03(42)
V_{NNN}	−5.68(2)	−5.23(3)	−0.45(3)
$V_{NC}=v_{NN}+V_{NNN}$			−1.48(42)
$E_{NC}^{internal}=T_{NC}^{internal}+V_{NC}$	−24.55(6)	−27.73(2)	3.18(6)

$=1.98(1)$ MeV is repulsive while $\langle V_{\Lambda NN}^{2\pi}\rangle=-2.41(2)$ MeV is found to be attractive and significant. We also note a small $\langle V_{\Lambda NN}^{2\pi}\rangle=0.16(1)$ MeV for pure Jastrow wave function ($U_{ij}=U_{ij}^{LS}=U_{ijk}=U_{ijk}^{TNI}=U_{\Lambda j}=U_{\Lambda jk}=0$). Thus, the noncentral correlations are responsible for the significant enhancement in the $\langle V_{\Lambda NN}^{2\pi}\rangle$. This may be understood with the consideration that $X_{i\Lambda}$ as given in Eq. (15) may be written as generalized tensor operators S_{12}, whose expectation value in a Jastrow wave function for a closed shell nucleus is zero but $\langle S_{12}^2\rangle$ is nonzero. We thus note that the value $\langle V_{\Lambda NN}\rangle$ is correlation dependent. Similar results were obtained for $^{17}_{\Lambda}$O hypernucleus [11].

The complete energy breakdown for $W_0=0.012$ MeV and $C_p=0.75$ MeV is reported in Table VI. For any other combination of strengths the energy breakdown except for $\langle V_{\Lambda NN}^{D}\rangle$ and $\langle V_{\Lambda NN}^{2\pi}\rangle$ will remain the same as we readjust the ΛNN correlation parameters for an optimal wave function as given in Eq. (45). In this case, we find $B_\Lambda=3.11(4)$ MeV, which is very close to the experimental value. In the same table, we also report on the energy breakdown for $W_0=C_p=0$, which means that both ΛNN potential and correlation are turned off. In this case, the hypernucleus is found to be overbound by 0.56(4) MeV, and the optimal value of $\alpha_{2\pi}^{\Lambda}$ is 0.95 instead of 0.935 and of long range ΛN asymptotic correlation parameter $\kappa_{\Lambda N}$ is 0.024 fm^{-1}, which is quite large compared to its previous value 0.008 fm^{-1} for the full wave function.

The nuclear energy of $^{5}_{\Lambda}$He is $-22.18(6)$ MeV with $U_{\Lambda ij}$ and $-21.62(6)$ MeV with no $U_{\Lambda ij}$. The little disagreement between these two values suggests that the effect of $U_{\Lambda ij}$ to the nuclear energy is weak.

The realistic NN, NNN, and ΛN potentials along with their corresponding correlations give small overbinding by at least a quarter of previous predictions of 2–3 MeV [29]. However, we do require ΛNN force to resolve this small overbinding. This also warrants that if such a realistic study is performed over a wide spectrum of hypernuclei to determine the ΛNN potential strengths, the *enigma* [1,30] of overbinding of $^{5}_{\Lambda}$He, on account of the use of central forces, will not survive.

C. Densities and polarization of ^{4}He core

In order to calculate the polarization energy of the core nucleus due to presence of Λ, we calculate the internal energy $E_{NC}^{internal}$, of the $(A-1)$ subsystem in the hypernucleus. Therefore, we duly take into account the center of mass (c.m.) motion of the subsystem and write down the internal kinetic energy of the core nucleus as given below,

$$T_{NC}^{internal}=\sum_{i=1}^{A-1}\frac{p_i^2}{2m}-\frac{\left(\sum_{i=1}^{A-1}p_i\right)^2}{2(A-1)m}\equiv T_{NC}-T_{NC}^{cm}, \quad (46)$$

where T_{NC}^{cm} represents the kinetic energy due to c.m. motion of $(A-1)$ subsystem around the c.m. of hypernucleus and T_{NC} is the nuclear kinetic energy of $^{5}_{\Lambda}$He as given in Table VI.

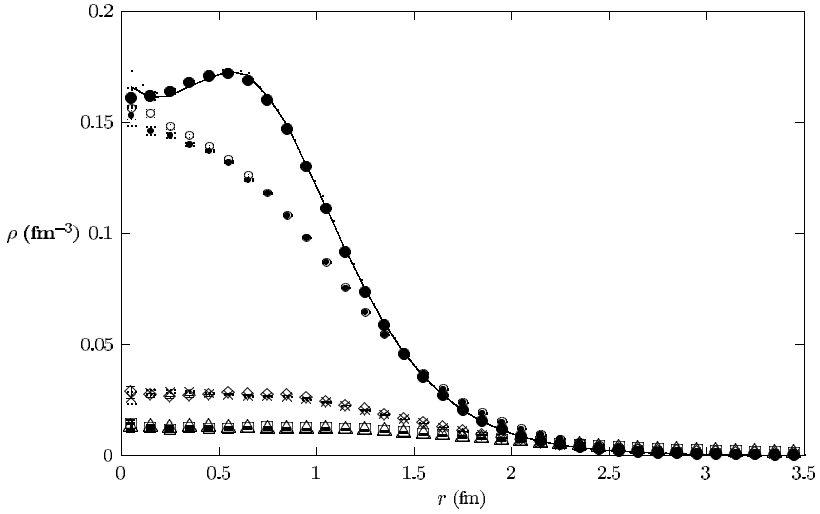

FIG. 3. One-body densities for N and Λ. The solid circles represent the nucleon density in isolated ^{4}He nucleus. The small filled (open) circles represent nucleon density and diamonds (cross points) represent Λ density in $^{5}_{\Lambda}$He with (without) $U_{\Lambda NN}$ correlation, respectively. Similarly, solid (dotted) line represents nucleon density and squares (triangles) represent Λ density in NC (meaning that c.m. of $4N$ subsystem is treated as the c.m. of hypernucleus) with (without) $U_{\Lambda NN}$ correlation, respectively.

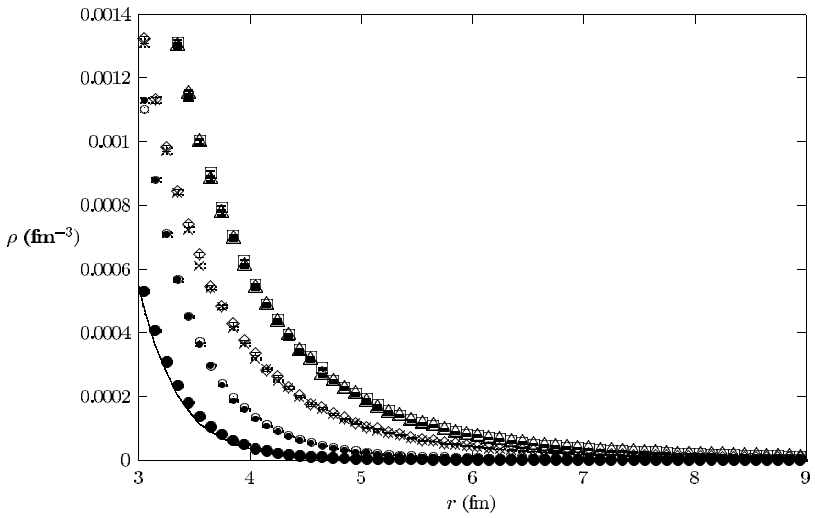

FIG. 4. One-body densities for N and Λ at peripheral region. The description of the plots are the same as in Fig. 3.

We compare the energy breakdown for ^{4}He and NC of $^5_\Lambda$He in Table VII. A total polarization of 3.18(6) MeV is noticed, which is about 0.8 MeV per nucleon. This value is significant. A similar effect was also observed for $^{17}_\Lambda$O, in which case the polarization of 11 MeV was noticed [11], which is about 0.7 MeV per nucleon. In this study and also in the study of ^{16}O [28] under CMC approach using v_6, the ground state energies are underestimated to about 20% of the experimental values. We believe that the NC polarization is also underestimated in the same proportion. A simple extrapolation gives a polarization of about 13–14 MeV, which is about 0.8–0.9 MeV per nucleon. Thus our results are consistent and are in good agreement with the findings of Ref. [11]. We also observe that the polarization is mainly in the kinetic energy of the NC, which is found to be 4.66(42) MeV. In the potential energy, polarization is $-1.48(43)$ MeV. Recently, Nemura, Akaishi, and Suzuki [30] have performed calculations of s-shell hypernuclei by explicitly including Σ degree of freedom. They do report on a large NC polarization energy. Our value is in the range discussed in their reported work.

The density profiles for nucleon and Λ are plotted in Figs. 3 and 4. The solid circles represent the nucleon density in isolated ^{4}He nucleus. The small filled (open) circles represent nucleon density and diamonds (cross points) represent Λ density in $^5_\Lambda$He with (without) $U_{\Lambda NN}$ correlation, respectively. Similarly, solid (dotted) line represents nucleon density and squares (triangles) represent Λ density in NC with (without) $U_{\Lambda NN}$ correlation, respectively. We obtain this when we take the c.m. of $4N$ subsystem as the c.m. of the hypernucleus. We also note that $U_{\Lambda NN}$ leads to a depression in densities at small r for every case. This is because of the repulsive piece of this correlation, which is due to repulsive $V^D_{\Lambda NN}$.

Most of the time Λ hyperon is found in the interior region near the center, and it pushes away the nucleons towards low density regions both at the periphery and in the center of the hypernucleus. As a result, the hole in the nucleon density distribution at the center in case of ^{4}He disappears. No density hole is seen at the center for Λ. In Fig. 4, we plot the one-body density distributions at peripheral region. The description of the various plots of this figure is the same as in Fig. 3. The nucleon density is found to vanish at 5.0 fm and 5.5 fm for ^{4}He and for $^5_\Lambda$He, respectively. However, Λ density survives until 8.5 fm. This long-range behavior suggests a Λ halo around the NC of the hypernucleus.

The effect of $U_{\Lambda NN}$ is small. We also note that u^Λ_σ is a very weak correlation to exhibit a significant effect on a physical observable. Therefore, we infer that the change in the nucleon density profile in the hypernucleus is due to the repulsive f^Λ_c correlation.

V. CONCLUSIONS

In this microscopic study, we observe that the realistic NN (AV18) and NNN (Urbana-IX) potentials in conjunction with ΛN and ΛNN potentials, give a good account of the experimental B_Λ value. We also note that without inclusion of ΛNN potential, the hypernucleus is overbound by 0.56(4) MeV, which is small compared to the earlier predictions of 2–3 MeV due to central forces. Still in such a realistic study we inevitably require the three-body ΛNN force to resolve the overbinding problem. However, in order to determine the two strengths W_0 and C_p of this potential, one must study a wide spectrum of hypernuclei in a similar way. The nuclear core polarization is found to be sufficiently large which is about 0.8 MeV per nucleon. This result is found to be in line with the findings of Ref. [11]. Also, the Λ hyperon density is found to be maximum near the center from where it pushes the nucleons towards the low density regions both at the periphery and at the center. A Λ halo structure is also seen. The change in nucleon density in NC compared to that of ^{4}He is certainly because of the f^Λ_c repulsive correlation.

For future studies, we suggest the inclusion of exchange ΛN correlation in the variational wave function. Though negligibly small, the s-wave $\pi\Lambda$ interaction should also be included in the ΛNN three-body force for the sake of completeness. One should also include Illinois realistic models of three-nucleon interactions [31], which give overall better results in comparison with the Urbana-IX one, specially for nuclei with large A and $N \neq Z$.

ACKNOWLEDGMENTS

A.A.U. is grateful to Steven C. Pieper for help since the beginning of this work and is thankful to R. B. Wiringa for giving his ^{4}He FORTRAN code which has been crucial for this study. He is also grateful to J. Narlikar for extending facilities at IUCAA, and S. H. S. Rizvi for constant encouragements. Finally, financial support through Grant No. SP/S2/K-32/99 sanctioned to him under SERC scheme, Department of Science and Technology, Government of India, is highly acknowledged.

[1] B.F. Gibson and E.V. Hungerford, III, Phys. Rep. **257**, 349 (1995).
[2] R.H. Dalitz, R.C. Herndon, and Y.C. Tang, Nucl. Phys. **B47**, 109 (1972).
[3] A.R. Bodmer and Q.N. Usmani, Nucl. Phys. **A477**, 621 (1988).
[4] A.R. Bodmer, Q.N. Usmani, and J. Carlson, Phys. Rev. C **29**, 684 (1984).
[5] Q.N. Usmani, Nucl. Phys. **A340**, 397 (1980).
[6] A. Gal, Adv. Nucl. Phys. **8**, 1 (1975).
[7] E.V. Hungerford and L.C. Biedenhorn, Phys. Lett. **142B**, 232 (1984).
[8] B. Povh, Prog. Part. Nucl. Phys. **5**, 245 (1980).
[9] H. Bando and I. Shimodaya, Prog. Theor. Phys. **63**, 1812 (1980).
[10] S. Shinmura, Y. Akaishi, and H. Tanaka, Prog. Theor. Phys. **71**, 546 (1981).
[11] A.A. Usmani, S.C. Pieper, and Q.N. Usmani, Phys. Rev. C **51**, 2347 (1995).
[12] A.A. Usmani, Phys. Rev. C **52**, 1773 (1995).
[13] R.B. Wiringa, V.G.J. Stoks, and R. Schiavilla, Phys. Rev. C **51**, 38 (1995).
[14] B.S. Pudliner, V.R. Pandharipande, J. Carlson, S.C. Pieper, and R.B. Wiringa, Phys. Rev. C **56**, 1720 (1997).
[15] B.S. Pudliner, V.R. Pandharipande, J. Carlson, and R.B. Wiringa, Phys. Rev. Lett. **74**, 4396 (1995).
[16] J. Carlson, V.R. Pandharipande, and R.B. Wiringa, Nucl. Phys. **A401**, 59 (1983).
[17] I.E. Lagaris and V.R. Pandharipande, Nucl. Phys. **A359**, 331 (1981).
[18] Q.N. Usmani and A.R. Bodmer, Phys. Rev. C **60**, 055215 (1999); Nucl. Phys. **A639**, 147c (1998).
[19] Q. N. Usmani, M. Sami, and A. R. Bodmer, in *Condensed Matter Theories*, edited by J. W. Clark, K. A. Shoeb, and A. Sadiq (Nova Science, Commack, NY, 1994), Vol. 9.
[20] A.R. Bodmer and Q.N. Usmani, Phys. Rev. C **31**, 1400 (1985).
[21] A.R. Bodmer, D.M. Rote, and A.L. Mazza, Phys. Rev. C **2**, 1623 (1970); J. Law, M. R. Gunye, and R. K. Bhaduri, in *Proceedings of the International Conference on Hypernuclear Physics*, edited by A. R. Bodmer and I. G. Hymen (Argonne National Laboratory, Argonne) (unpublished), p. 333.
[22] A.R. Bodmer and D.M. Rote, Nucl. Phys. **A169**, 1 (1971).
[23] J. Rozynek and J. Dabrowski, Phys. Rev. C **20**, 1612 (1979); **23**, 1706 (1981); Y. Yamamoto and H. Bando, Prog. Theor. Phys. Suppl. **81**, 9 (1985); Y. Yamamoto, Nucl. Phys. **A450**, 275c (1986).
[24] R.K. Bhaduri, B.A. Loiseau, and Y. Nogami, Ann. Phys. (N.Y.) **44**, 57 (1967).
[25] A. Arriaga, V.R. Pandharipande, and R.B. Wiringa, Phys. Rev. C **52**, 2362 (1995).
[26] R.B. Wiringa, Phys. Rev. C **43**, 1585 (1991).
[27] R.B. Wiringa, S.C. Pieper, J. Carlson, and V.R. Pandharipande, Phys. Rev. C **62**, 014001 (2000).
[28] S.C. Pieper, R.B. Wiringa, and V.R. Pandharipande, Phys. Rev. C **46**, 1741 (1992).
[29] See, for example, Ref. [2] and references therein.
[30] H. Nemura, Y. Akaishi, and Y. Suzuki, Phys. Rev. Lett. **89**, 142504 (2002).
[31] S.C. Pieper, V.R. Pandharipande, R.B. Wiringa, and J. Carlson, Phys. Rev. C **64**, 014001 (2001).